Arabian Journal of Chemistry 16 (2023) 105310

Contents lists available at ScienceDirect

Arabian Journal of Chemistry

journal homepage: www.sciencedirect.com

Original article

Low-cost and highly thermally conductive silver modified mica-paraffin multifunctional composite phase change materials for photo-thermal conversion and electrical insulation

Cheng Pan [a,b,*], Xiaofei Li [b], Guozhi Fan [a], Haitao Yang [b], Yifei Long [a], Feifan Wu [b]

[a] School of Chemical and Environmental Engineering, Wuhan Polytechnic University, Wuhan 430023, China
[b] Hubei Provincial Key Laboratory of Green Materials for Light Industry, Hubei University of Technology, Wuhan 430068, China

ARTICLE INFO

Article history:
Received 24 April 2023
Accepted 21 September 2023
Available online 26 September 2023

Keywords:
Phase change material
Modified mica
Solar thermal conversion

ABSTRACT

To improve the utilization efficiency of renewable energy and adaptability of composite materials, a new mineral-based composite phase change material (Ag-Mica/CNF/PW) was designed and prepared by chemically modifying natural mica, attaching silver nanoparticles to the mica surface as functionalized support material, and using paraffin wax as the phase change functional medium. As expected, the thermal conductivity of the composite phase change material (CPCMs) increased significantly to 0.9 W/m k, which was 330.1% higher relative to pure paraffin. With the addition of silver-modified mica, the volume resistivity of CPCMs reached 11.9 × 10^{12} Ω cm. The relative enthalpy efficiency achieved 104.8%, and the photothermal conversion efficiency reached 91.3%, proving that the silver-modified mica-based CPCM was successful and feasible. The heat resistance index of CPCMs was 137.2 °C, and the enthalpy loss rate after 50 cycles was only 0.7 %, indicating that CPCMs have excellent thermal stability. The designed CPCMs are a promising candidate for developing thermal storage and building thermal management, electrical insulation and solar energy conversion.

1. Introduction

With the continuous consumption of fossil fuels, it is particularly urgent to find a suitable alternative resource. Solar energy is one of the resources that can be used, but it is currently an important issue to improve its utilization efficiency. Thermal energy storage (TES) uses storage media to store and release thermal energy when needed (Kou et al., 2021). It has been recognized as one of the most effective ways to improve energy efficiency and alleviate the contradiction between energy supply and demand. Phase-change materials (PCMs) are a class of materials that can undergo phase change in response to changes in the external environment temperature, and store and release heat during the phase change process.

However, PCMs such as paraffins, fatty acids and polyols suffer from certain disadvantages in thermal management applications, such as easy leakage of the phase change processes. To solve the leakage problem of PCMs, porous support materials such as metal–organic framework (Atinafu et al., 2022), Hierarchical porous carbon (Li et al., 2022), attapulgite, and montmorillonite (Gao et al., 2022) were integrated to form a stable PCM. Mineral-based PCMs have been extensively investigated to solve the problem of leakage based applications of phase change materials because of their large specific surface area, low cost, easy availability, and high chemical stability. The addition of mineral-based materials inevitably affects the latent heat, thermal conductivity, mechanical strength and other properties of composite phase change materials. Based on this, techniques such as functional filler modification treatment (Jiang et al., 2021) and organic intercalation (Liu and Yang, 2014) were used to improve the latent heat of CPCMs, and means such as in situ growth of high thermal conductivity materials on mineral-based surfaces (Xu et al., 2021) and physical co-blending (Zhang et al., 2019) were used to enhance the thermal conductivity of composite phase change materials. Compared with metallic nickel, aluminum and copper (Wang et al., 2022), the application of silver in the CPCMs system is not only reflected in the thermal conductivity, but more importantly,

* Corresponding author.
E-mail address: ch_pan1018@whpu.edu.cn (C. Pan).
Peer review under responsibility of King Saud University.

Production and hosting by Elsevier

https://doi.org/10.1016/j.arabjc.2023.105310
1878-5352/

it has excellent photothermal conversion properties, which can improve the photothermal conversion capacity of the CPCM and play an important role in the efficient utilization of solar energy resources.

Based on this, a low-cost, high manufacturing efficiency and scalable vacuum impregnation method was used to design and prepare chemically silver-modified mineral-based mica-loaded paraffin composites. The structural and thermal storage properties of the composites were investigated, and the CPCMs exhibited excellent relative latent heat energy and stability. In addition, paraffin (PW) was filled into the network formed by physical mixing of mica and CNF, which effectively avoided inhomogeneity and leakage problems. This study provides ideas for the rational design of CPCMs for thermal storage and building thermal management, electrical insulation and photothermal conversion.

2. Experimental

2.1. Materials

Mica (800 mesh) was obtained from Guangxi province China. Sigma Aldrich provided novel cellulose nanofibers (CNFs) (Carboxyl content of 0.07%) (Shanghai, China). Sinopharm Chemical Reagent Co. Ltd. provided boron nitride (BN), paraffin (PW), silver nitrate and ammonia (Shanghai, China). The materials and chemicals can be used without further purification.

2.2. Preparation of CPCM (Ag-Mica/CNF/PW)

In order to prepare Ag-Mica, silver was deposited on the surface of mica via silver mirror reaction. After desiccation, the Ag-Mica

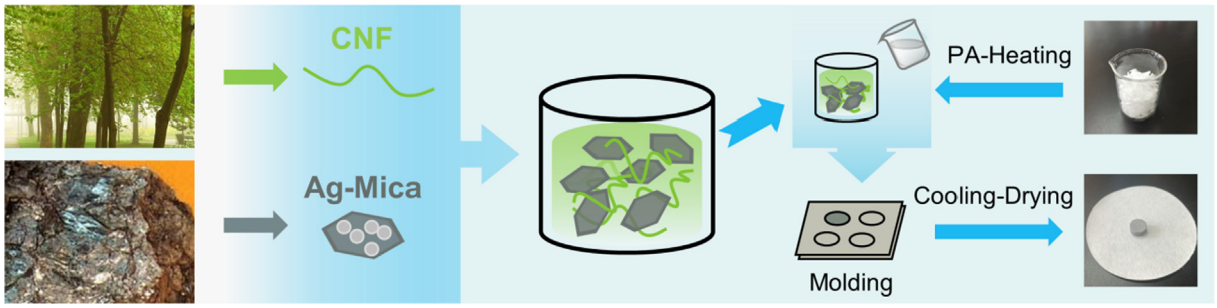

Scheme 1. Schematic representation for the preparation process of Ag-Mica/CNF/PWx.

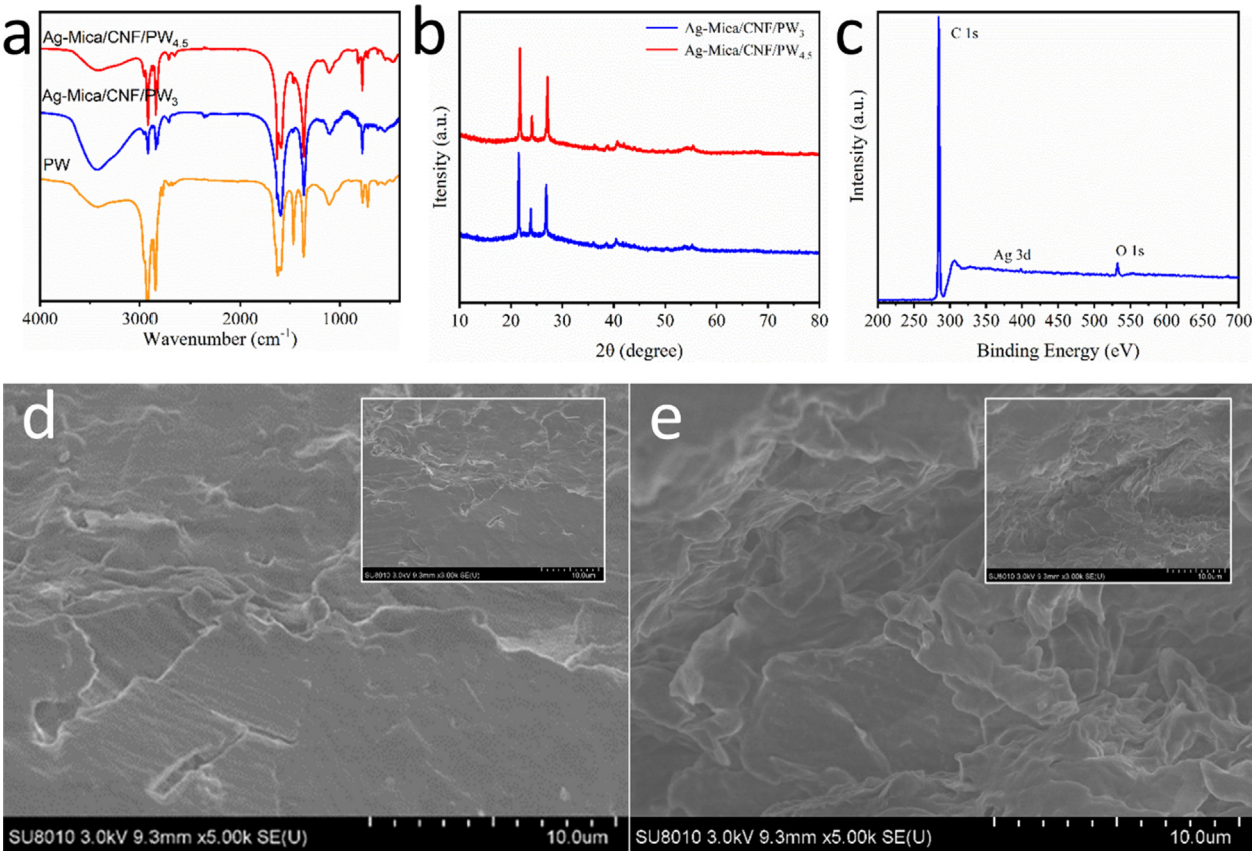

Fig. 1. (a)FT-IR, (b)XRD, (c)XPS, SEM image of the Ag-Mica/CNF/PW_3 (d) and Ag-Mica/CNF/$PW_{4.5}$ (e) (inset is low multiples).

was prepared. In a typical preparation procedure (Scheme. 1), Ag-Mica and boron nitride (BN) were dispersed in CNF suspensions (1 wt%), sonicated for 1 h. Subsequently, 2 g of PW in the beaker was heated to melt at 85 °C and mixed with as-prepared materials (Ag-Mica/CNF_x) in combination. Finally, the above carrier and PCM were fully mixed evenly under vacuum at 80 °C by vacuum

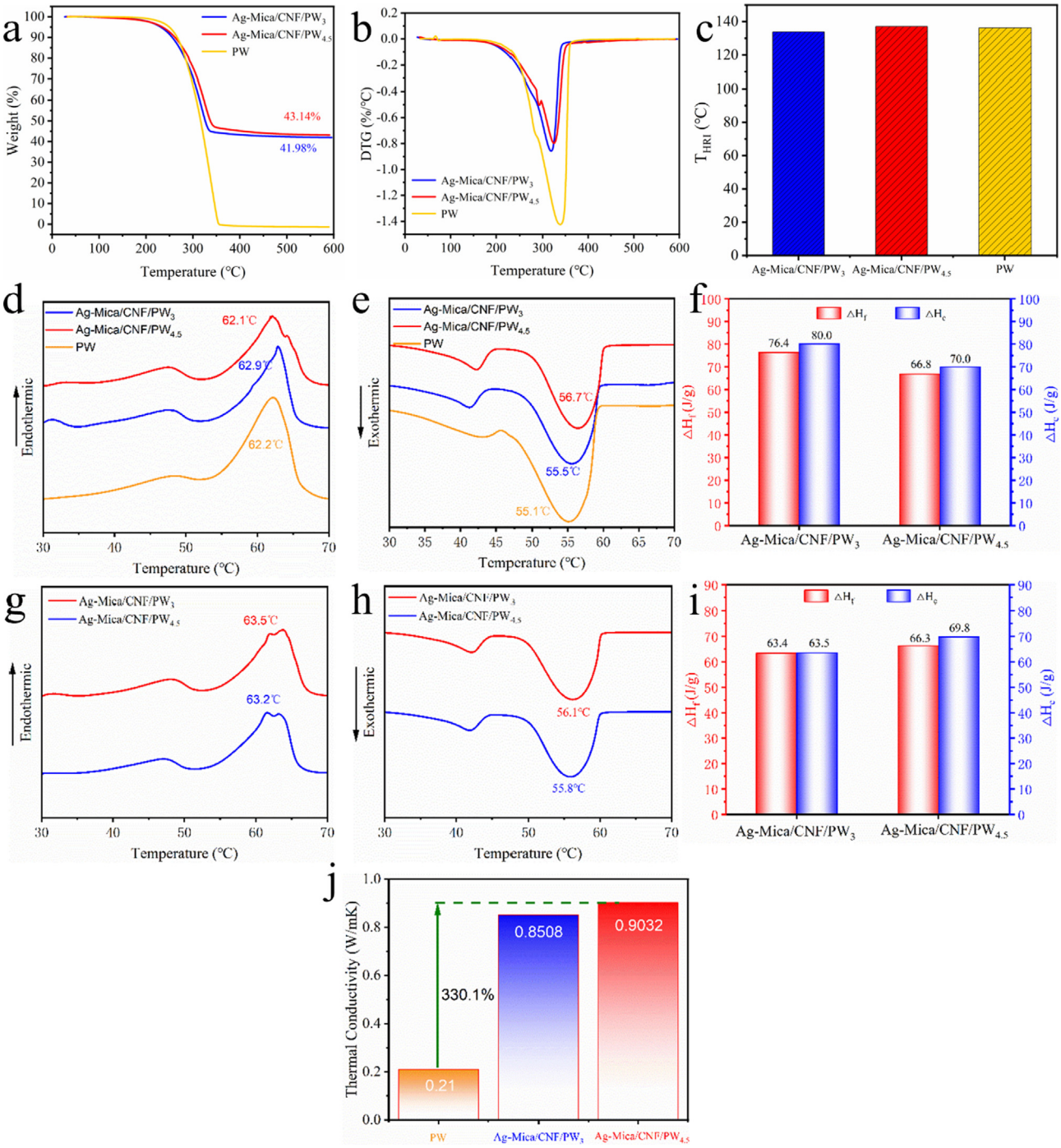

Fig. 2. (a-c) TGA, (d-e) DSC of CPCMs, (f) melting and freezing latent heat, (g-i) DSC 50 cycling, (j) Thermal conductivity of PW and CPCMs.

Table 1
Thermal parameters of the pure PW and CPCMs before cycling.

Samples	Melting process		Crystallization process			Relative enthalpy efficiency
	Enthalpy (J/g)	T_f (°C)	Enthalpy (J/g)	T_c (°C)	ω (%)	η
PW	125.6	62.2	124.4	55.1	100	
Ag-Mica/CNF/PW_3	76.4	62.9	80.0	55.5	58.0	104.8
Ag-Mica/CNF/$PW_{4.5}$	66.8	62.1	70.0	56.7	56.9	93.5

impregnation method. Immediately afterwards, the mixture was rapidly poured in the mold to create a cylinder-shaped form-stable CPCMs, referred to as Ag-Mica/CNF/PW_3 and Ag-Mica/CNF/$PW_{4.5}$, corresponding to CNF suspensions (1 wt%) (3 g and 4.5 g).

2.3. Characterization

The molecular structures of the CPCMs were identified by a Fourier transform infrared (FT-IR) spectrometer (Bruker, Karlsruhe, Germany) using KBr pellet technology in the wavelength range of from 4000 cm^{-1} to 400 cm^{-1}. X-ray photoelectron (XPS) spectra were acquired on an Thermo Scientific K-Alph spectrometer to explore the valence state of C, O, and Ag under the working voltage of 12 kV. The crystal structures of CPCMs using a Bruker D8 advance X-ray diffractometer (XRD) at an operating voltage of 40 kV and a current density of 40 mA in the 2θ range of 10-80°. The morphology and microstructure of the CPCMs were examined by scanning electron microscopy (Zeiss Merlin, Oberkochen, Germany) at an accelerating voltage of 10 kV. Thermogravimetric analysis (TGA) was conducted in a thermogravimetric simultaneous thermal analyser (PerkinElmer STA 8000) to evaluate thermal stability and load of CPCMs in the temperature range of 25 °C to 600 °C with a heating rate of 10 °C/min, in a nitrogen atmosphere. Differential scanning calorimetry (DSC, TA Q2000) was used to test the thermal property parameters of PW and CPCMs, such as phase transition temperature, latent heat value, from 30 °C to 70 °C in N_2 atmosphere at a heating/cooling rate of 5 °C. The thermal conductivity of CPCMs was measured with a transient planar heat source thermal conductivity meter (Hot Disk TPS 2500S). The thermal infrared image and temperature variation of PW and CPCMs during heating/cooling were recorded by the thermal infrared imaging device. The resistivity of CPCMs were measured by an ultra-high resistance tester (ST2643) and a standard ring triple electrode. Image recording of morphology stability of CPCMs were obtained by a mobile camera. The light thermal conversion performance of CPCMs was investigated utilizing a photothermal conversion simulation device composed of a xenon lamp light source (CEL-HXF300), a k-type thermocouple, a data logger M2101-SDS1011 and a computer (Pan et al., 2023).

3. Results and discussion

3.1. Morphology and crystalline structure of composites

The FT-IR analyzer was used to detect the functional groups in the composite phase change materials of PW, Ag-Mica/CNF/PW_3 and Ag-Mica/CNF/$PW_{4.5}$, as shown in Fig. 1a. The FT-IR spectra revealed the intensities of the typical paraffin bands at 2927, 2852, 1463, 1365, 773 and 721 cm^{-1}, assigned to the symmetrical stretching vibration of the $-CH_3$ group, $-CH_2$, deformation vibration of $-CH_2$ and $-CH_3$ groups, and $-CH_2$ rocking vibration, respectively (Baglioni et al., 2018). In addition, the band at 3446 cm^{-1} was symmetrical stretching vibration of –OH groups. According to the infrared spectrum analysis of paraffin and two composite phase change materials, the characteristic bands of PW also appeared in Ag-Mica/CNF/PW composite phase change materials. The characteristic bands of the components were present in case of the composites, indicating that the materials were successfully and completely compounded and that the mixing did not change the chemical structure of PW.

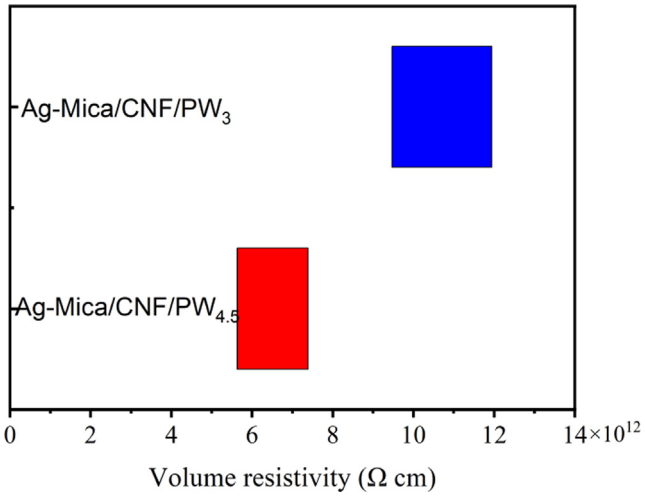

Fig. 3. Volume resistivity of Ag-Mica/CNF/PW_3 and Ag-Mica/CNF/$PW_{4.5}$.

X-ray diffractometry (XRD), using an X-ray diffractometer, was also performed to determine the crystal phase of composite phase change materials. As illustrated in Fig. 1b, two strong and sharp diffraction peaks at 21.8° and 24.1° were characteristic peaks of PW (Hu et al., 2022), which went up with the increase of PW content in the mica-doped compo-sites. The characteristic peak at 38.7° corresponds to the (1,1,1) plane of cubic Ag crystal, indicating that Ag nanoparticles were successfully plated on the surface of mica (Xiao et al., 2022a). The diffraction pattern for CPCMs exhibited a distinct peak at 26.8°, a characteristic of mica Ilic et al., 2016. The diffraction peaks of the two samples were basically the same except for the intensity, and the position of the diffraction peaks did not move significantly, indicating that the chemical structure of the composites with different contents remained consistent, and the compounding process did not change the properties of the components. This result is consistent with the FTIR results. The elemental composition of Ag-Mica/CNF/$PW_{4.5}$ was analyzed using XPS. The results demonstrated that the main elements in

Table 2
Comparison of CPCMs in this work and previous literatures.

	Thermal conductivity enhancement (%)	Thermal conductivity (W/m K)	Reference
Paraffin/SiO2 + EG	19.05	0.25	Zhang et al., 2012
Heptadecane(18 wt%) /bentonite + EG	166.67	0.56	Karaman et al., 2011
PW-SBS/CNT-85	85.71	0.39	Hu et al., 2022
HPC 2.0-PW	57.14	0.33	Sun et al., 2020
C-900/PW	66.67	0.35	Wang et al., 2017
PEG/BPC-Ag	200.00	0.63	Xiao et al., 2022a
Carbonized BPC/nano-Ag	204.76	0.64	Xiao et al., 2022b
PEG-EP/EG-Ag	214.29	0.66	Luo et al., 2022
Ag-Mica/CNF/PW_3	304.76	0.85	This work
Ag-Mica/CNF/$PW_{4.5}$	328.57	0.90	This work

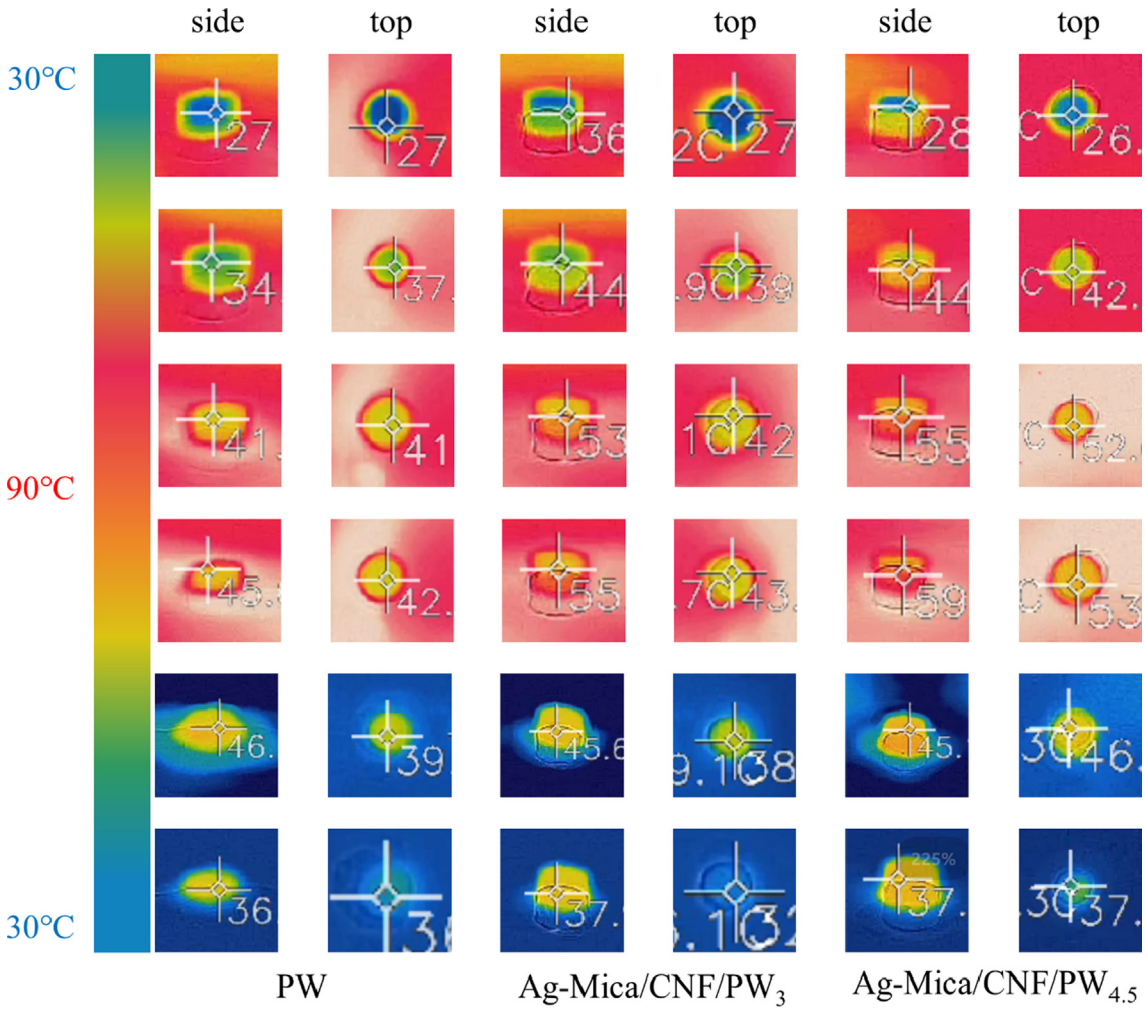

Fig. 4. Heating and cooling IR images of PW and CPCMs.

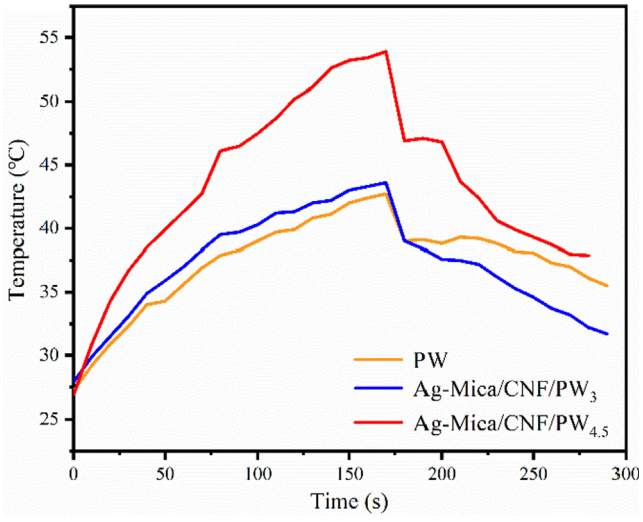

Fig. 5. Temperature variations and phase change evolution during heating and cooling process.

the CPCMs were C, O and Ag, as shown in Fig. 1c. The element C was derived not only from paraffin, but also from a small amount of nanocellulose (CNF). The results show that the O element signal comes from mica and CNF.

The microstructure of CPCMs was observed by SEM after vacuum impregnation of silver-modified mica with paraffin wax. The results are shown in Fig. 1d-e. The multilayer stacked lamellar structure of mica did not change after silver modification, and the morphology remained stable after loading the paraffin phase change material. The interstices of the lamellar structure of mica mineral carriers could well adsorb and fill the phase change material, and this pore structure provided a reliable support skeleton for the composite phase change material, so that the phase change material maintained a stable shape during the melting process without the leakage of PW. At the same time, we found that the mineral-based filler and PW were well combined, and the CPCM with uniform composition was prepared.

3.2. Thermal stability and phase change behaviour

The thermal stability of CPCMs and PW was studied via thermogravimetric analysis. The TGA curves of the samples (Fig. 2a) showed no distinct decomposition reaction or mass loss from 25 °C to 150 °C, which were much lower than this value in daily use, indicating that Ag-Mica/CNF/PW showed the excellent thermal stability. The thermal stability of the spun film was evaluated according to the heat resistance index (T_{HRI}), which can be calculated by its degradation temperature ($T_{5\%}$ and $T_{30\%}$) (Liu et al., 2022, Pan et al. 2023). The T_{HRI} (Fig. 2c) of Ag-Mica/CNF/PW_3 and Ag-Mica/CNF/$PW_{4.5}$ were 136.8 °C and 137.2 °C, respectively,

Fig. 6. Digital images of CPCMs thermal leakage experiments.

which were higher than pure PW (136.1 °C). This indicated the excellent thermal stability of the CPCMs. Compared with pure PW, the maximum loss rate of CPCMs was lower (Fig. 2b), indicating that the mica/polymer mixture with high diameter-thickness ratio had excellent thermal stability. It was determined from the mass loss of the samples, which can be calculated from the graphs as 58.0 % and 56.9 % for Ag-Mica/CNF/PW_3 and Ag-Mica/CNF/$PW_{4.5}$ loadings respectively by TGA testing.

The phase change latent heat value is a key property of composite phase change energy storage materials, representing the heat storage capacity of the sample. The DSC curves for the CPCMs and PW were illustrated in Fig. 2(d-f), and both have two similar phase change peaks, the melting peak and the freezing peak, respectively, which means that the crystallisation process of PW was not changed. There was no chemical reaction involved in the mixing of PW during the vacuum impregnation process. In addition, the phase transition characteristic data including melting temperature (T_f), melting enthalpy (ΔH_f), crystallization temperature (T_c), and crystallization enthalpy (ΔH_c) measured by the DSC curve were shown in Table 1. The value of η (relative enthalpy efficiency) was usually used to evaluate the heat storage capacity of CPCM (Sun et al., 2018, Luo et al., 2021). The value of η was obtained according to the eq. (1), the greater the value of η indicated the heat storage performance of CPCM.

$$\eta = \frac{\Delta H_f(CPCM)}{\Delta H_f(PW) \times \omega} \times 100\% \quad (1)$$

where $\Delta H_f(CPCM)$ is the melting enthalpy of the CPCM, $\Delta H_f(PW)$ is the melting enthalpy of polyethylene glycol, and ω indicates the weight fraction of paraffin in the CPCM sample. By calculation, the η of Ag-Mica/CNF/PW_3 and Ag-Mica/CNF/$PW_{4.5}$ were 104.8 % and 93.5 % respectively. The above results illustrates that the prepared CPCM using the CNF grafting has good thermal storage properties. The phase change stability of CPCM is one of the most critical factors in practical applications. Therefore, to measure the reversibility of the thermal reliability of CPCMs, a 50-cycle DSC test (Fig. 2g-i) was performed to confirm the extent of latent heat loss during repeated phase changes (Yuan et al., 2022). The transformation temperature of all samples occurred with a slight downshift. Compared with Ag-Mica/CNF/PW_3, the enthalpy loss rate of Ag-Mica/CNF/$PW_{4.5}$ after 50 cycles was relatively low, only 0.7 %. In summary, the composite phase change material has good thermal stability and reusability.

The thermal conductivity of CPCM samples at room temperature was measured by a thermal conductivity meter. The highest thermal conductivity was obtained for the Ag-Mica/CNF/$PW_{4.5}$ in Fig. 2j, the value of 0.90 W/m K corresponds to an improvement of 328.57 % compared with that of the pure (0.21 W/m K) and Ag-Mica/CNF/$PW_{4.5}$ (0.85 W/m K). The reason was that the silver nanoparticles attached to the mica surface provided more additional heat transfer channels for CPCMs, accelerating the heat transfer and thus further improving the thermal conductivity. Among them, the comparison of the thermal conductivity of CPCMs obtained in this study with other nanoparticle-modified carriers in related papers was shown in Table 2, which indicated that the thermal conductivity of the samples was significantly better than those of other studies, further proving the effectiveness and novelty of the carrier selected in this work.

The electrical properties of Ag-Mica/CNF/PW_3 and Ag-Mica/CNF/$PW_{4.5}$ were analysed to verify their enormous potential as insulating high thermal conductivity PCM composites. Based on the bulk resistivity spectra of the composites (Fig. 3), the CPCMs exhibited excellent insulating properties with a maximum bulk resistivity of 11.9×10^{12} Ω cm and an overall maintenance of the order of 10^{12} Ω cm. The aforementioned results indicate that the mica-doped PCM composite have a promising application as electrical insulation material.

As shown in Fig. 4, to characterize the thermal management performance of CPCMs, CPCMs and PW were heated on a hot plate at 90 °C for 3 min and then removed and cooled at ambient temperature. Throughout the heating and cooling process, the side and top face of cylindrical shape samples were photographed with a fixed infrared thermal imaging camera. During the heating process, the temperature of CPCMs increased rapidly, and the colour of cylindrical samples changed from blue to red with the increase of heating time inthermal infrared imaging could also be clearly seen. Compared to the pure paraffin sample, the color of Ag-Mica/CNF/$PW_{4.5}$ changed more rapidly and showed red color more quickly, indicating that the heat transfer rate of Ag-Mica/CNF/$PW_{4.5}$ was faster. After removing the samples from the heating plate, the external ambient temperature in the thermal infrared imaging rapidly decreased, whereas CPCMs colour changed relatively slowly. This was because the heat stored in the CPCMs was slowly released and eventually dropped to room temperature. Meanwhile, the cylindrical shape of paraffin wax collapsed, and the shape of Ag-Mica/CNF/PW_3 and Ag-Mica/CNF/$PW_{4.5}$ did not change substantially and the cylindrical model structure was retained, indicating that the introduction of mineral mica carriers could limit the leakage of PCM well.

The melting and freezing performances were evaluated by temperature as time curves comparison of a molded tablet of CPCMs. The corresponding heating and freezing curves of the molded tablets of PW, Ag-Mica/CNF/PW_3 and Ag-Mica/CNF/$PW_{4.5}$ are

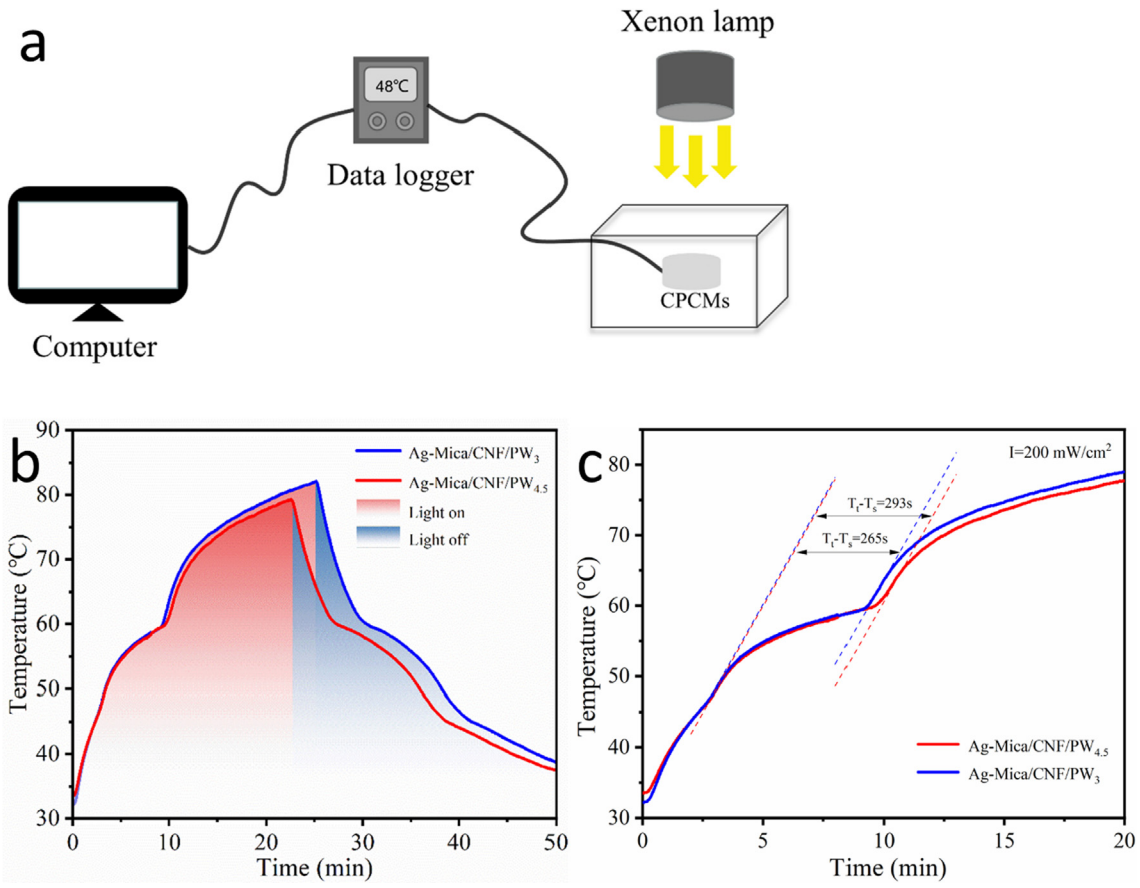

Fig. 7. (a) Schematic diagram of the experimental model; (b) Time-temperature profiles of the photo-thermal conversion process; (c) The value of T_t-T_s calculation schematic.

shown in Fig. 5, respectively. As can be seen, Ag-Mica/CNF/$PW_{4.5}$ rised to higher temperature during external heating and longer time and lower cooling rate to room temperature after stopping external heating, suggesting that the introduction of silver-loaded mica flakes greatly enhanced the thermal storage management capability of the composite phase change material. This conclusion is consistent with the above infrared thermographic observations.

In order to test the macroscopic thermal stability of the sample, the CPCM sample was placed on the heating plate for heating, starting from 30 °C, heating up 10 °C every 10 min and holding 10 min, and finally rising to 80 °C for 10 min, and the test results are shown in Fig. 6. The pure PW sample started to leak when it was heated to 60 °C at the beginning, and a large amount of leakage occurred after rising to 80 °C, and finally melted completely. However, under the same conditions, the Ag-Mica/CNF/PW_3 and Ag-Mica/CNF/$PW_{4.5}$ samples remained stable in shape without leakage until a small amount of leakage occurred at 80 °C. This indicates that the CPCM (Ag-Mica/CNF/PW) prepared by nanoparticle-modified mica has good thermal stability.

The energy conversion performance enables CPCMs to efficiently achieve fast visible light capture and photothermal energy conversion. The test setup as depicted in Fig. 7a, a xenon lamp source was used as the simulated sunlight source the Ag-Mica/CNF/PW_3 and Ag-Mica/CNF/$PW_{4.5}$, and a temperature sensor monitored temperature changes. The CPCMs temperature increased significantly as the lamp was turned on and decreased correspondingly as the lamp was turned off. From the Fig. 7b, it can be found that the maximum temperature of the Ag-Mica/CNF/PW sample can reach 82.1 ℃ under the same light condition, which was higher than the melting temperature of pure PW, proving that CPCMs has excellent photothermal conversion performance. Additionally, during the heating and cooling of CPCMs, two 'plateaus' appeared around 60 °C, which is consistent with the phase-transition temperature of the composites. This behaviour indicates that a large amount of thermal energy was released from CPCMs during the cooling process.

To accurately compare the photothermic conversion efficiency (φ) of the samples, the photothermic conversion efficiency of the samples was calculated by Eq. (2) (Fang et al., 2022; Lin et al., 2020)

$$\varphi = \frac{m\Delta H_f}{IS(T_t - T_s)} \tag{2}$$

where m and ΔH_f are the mass of the sample and the enthalpy of phase change of melting, respectively, I and S are the light intensity and light area, respectively, and T_s and T_t are the time points at

Table 3
Comparison of φ values for the Ag-Mica/CNF/PW with those for CPCMs in the relevant literature.

Samples	Photo-thermal conversion efficiency (φ) %	Reference
PW-CNTS	60.0	Chen et al., 2012
PEG-EP/EG-Ag	90.7	Luo et al., 2022
CW-2/OP44E	86.0	Pan et al., 2021
CPCM3	88.1	Xu et al., 2022
Ag-Mica/CNF/PW_3	91.3	This work
Ag-Mica/CNF/$PW_{4.5}$	82.5	This work

which the phase change starts and ends, respectively. Fig. 7c shows the temperature variation curves of the samples over 20 min. The photothermal conversion efficiencies of the Ag-Mica/CNF/PW_3 and Ag-Mica/CNF/$PW_{4.5}$ were calculated to be 91.3% and 82.5%, respectively. The results indicated that the composites obtained by using Ag-deposited mica as a carrier loaded phase change material have excellent photothermal conversion capability. Among them, the comparison of the thermal conductivity of CPCMs obtained in this study with other nanoparticle-modified carriers in related papers was shown in Table 3, which indicated that the thermal conductivity of the samples was better than those of other studies.

In summary, under the same light conditions, Ag-Mica/CNF/PW_x performed well in terms of solar energy conversion efficiency and heat energy release rate. It proves that the silver-modified mica-loaded phase change material scheme is successful and feasible. The above results indicate that mica-based composite phase change materials have potential in the field of solar energy utilization.

4. Conclusions

In this work, a new mineral-based Ag-Mica/CNF/PW composite phase change material was designed and prepared by chemically modifying natural mica, attaching silver nanoparticles as functionalized support material on the mica surface, and using paraffin wax as the phase change functional medium. With the addition of silver-modified mica, the thermal conductivity of the composites was significantly increased to 0.9 W/mK, which was 330.1% higher relative to pure paraffin. More surprisingly, due to the insulating properties of the mica mineral matrix, the volume resistivity of the composite phase change material reaches 11.9×10^{12} Ω cm. The thermal storage capacity of Ag-Mica/CNF/PW − η (relative enthalpy efficiency) achieved 104.8 %, which illustrates that the prepared composite phase change material using the CNF grafting has good thermal storage properties. The arrangement of layered structure and the uniform distribution of silver nanoparticles can improve the photothermal conversion efficiency of Ag-Mica/CNF/PW to 91.3%, which is higher than some reported literature, proving that the silver-modified mica-based composite phase change material is successful and feasible. In addition, the phase change performance of the composites in this study decreased less after 50 thermal cycles. TGA and thermal leakage test results showed that the layered structure of flaky mica can well fix the PCM inside the multi-layer structure, which made CPCMs had excellent thermal stability and reusability. In summary, it provides a wide range of large-scale application prospects in the field of thermal storage and building thermal management, electrical insulation and solar thermal storage.

The submission has been received explicitly from all co-authors. And authors whose names appear on the submission have contributed sufficiently to the scientific work and therefore share collective responsibility and accountability for the results.

Declaration of Competing Interest

The authors declare that they have no known competing financial interests or personal relationships that could have appeared to influence the work reported in this paper.

Acknowledgment

The authors are grateful for the support of the National Nature Science Foundation of China, China (NSFC, No. 21978074) and the key project of Hubei province, China (Grant No. 2022BCA081).

References

Atinafu, D.G., Yun, B.Y., Yang, S., et al., 2022. Updated results on the integration of metal–organic framework with functional materials toward n-alkane for latent heat retention and reliability. J. Hazard. Mater. 423,. https://doi.org/10.1016/j.jhazmat.20 21.127147 127147.

Baglioni, M., Poggi, G., Ciolli, G., et al., 2018. A triton x–100-based microemulsion for the removal of hydrophobic materials from works of art: saxs characterization and application. Materials 11, 1144. https://doi.org/10.3390/ma11071144.

Chen, L.J., Zou, R.Q., Xia, W., et al., 2012. Electro- and photodriven phase change composites based on wax-infiltrated carbon nanotube sponges. ACS Nano 6, 10884–10892. https://doi.org/10.1021/nn304310n.

Fang, Y., Liu, S., Li, X.L., et al., 2022. Biomass porous potatoes/MXene encapsulated PEG-based PCMs with improved photo-to-thermal conversion capability. Sol. Energ. Mat. Sol. Cells 237,. https://doi.org/10.1016/j.solmat.2021.111559 111559.

Gao, D.C., Sun, Y.J., Fong, A.M., et al., 2022. Mineral-based form-stable phase change materials for thermal energy storage: A state-of-the art review. Energy Storage Mater. 46, 100–128. https://doi.org/10.1016/j.ensm.2022.01.003.

Hu, D., Han, L., Zhou, W., et al., 2022. Flexible phase change composite based on loading paraffin into cross-linked cnt/sbs network for thermal management and thermal storage. Chem. Eng. J. 437,. https://doi.org/10.1016/j.cej.2022.135056 135056.

Ilic, B., Radonjanin, V., Malesev, M., et al., 2016. Effects of mechanical and thermal activation on pozzolanic activity of kaolin containing mica. Appl. Clay Sci. 123, 173–181. https://doi.org/10.1016/j.clay.2016.01.029.

Jiang, F., Ge, Z.W., Ling, X., et al., 2021. Improved thermophysical properties of shape-stabilized nano3 using a modified diatomite-based porous ceramic for solar thermal energy storage. Renew. Energy 179, 327–338. https://doi.org/10.1016/j.renene.2021.07.023.

Karaman, S., Karaipekli, A., Sar, A., et al., 2011. Polyethylene glycol (PEG)/diatomite composite as a novel form-stable phase change material for thermal energy storage. Sol. Energy Mater. Sol. Cells 95, 1647–1653. https://doi.org/10.1016/j.solmat.2011.01.022.

Kou, Y., Sun, K.Y., Luo, J.P., et al., 2021. An intrinsically flexible phase change film for wearable thermal managements. Energy Storage Mater. 34, 508–514. https://doi.org/10.1016/j.ensm.2020.10.014.

Li, Y.Q., Huang, X.B., Lv, J.J., et al., 2022. Enzymolysis-treated wood-derived hierarchical porous carbon for fluorescence-functionalized phase change materials. Compos. B Eng. 234,. https://doi.org/10.1016/j.compositesb.2022.109735 109735.

Lin, P.C., Xie, J.J., He, Y.D., et al., 2020. Mxene aerogel-based phase change materials toward solar energy conversion. Sol. Energy Mater. Sol. Cells 206,. https://doi.org/10.1016/j.solmat.2019.110229 110229.

Liu, Z., Fan, X., Han, M., et al., 2022. Branched fluorine/adamantane interfacial compatibilizer for synchronously enhancing interlaminar shear strength and wave-transparent performances of PBO fibers/cyanate ester laminated composites. Chin. J. Chem . 40, 939–950. https://doi.org/10.1002/cjoc.202200749.

Liu, S.Y., Yang, H.M., 2014. Composite of coal-series kaolinite and capric-lauric acid as form-stable phase-change material. Energy Technol. https://doi.org/10.1002/ente.201402125.

Luo, W.X., Hu, X.W., Che, Y.H., et al., 2022. Form-stable phase change materials enhanced photothermic conversion and thermal conductivity by Ag-expanded graphite. J. Energy Storage 52,. https://doi.org/10.1016/j.est.2022.105060 105060.

Luo, Y., Zhang, F., Li, C.C., et al., 2021. Biomass-based shape-stable phase change materials supported by garlic peel-derived porous carbon for thermal energy storage. J. Energy Storage 46,. https://doi.org/10.1016/j.est.2021.103929 103929.

Pan, C., Wu, F.F., Fan, G.Z., et al., 2023. A multifunctional flexible composite film with excellent insulation flame retardancy, thermal management and solar-thermal conversion properties based on CNF-modified mica/electrospun fibrous networks structure. Sol. Energy Mater. Sol. Cells 261,. https://doi.org/10.1016/j.solmat.2023.112530 112530.

Pan, X.Y., Zhang, N., Yuan, Y.P., et al., 2021. Balsa-based porous carbon composite phase change material with photo-thermal conversion performance for thermal energy storage. Sol. Energy 230, 269–277. https://doi.org/10.1016/j.solener.2021.10.046.

Sun, K.Y., Kou, Y., Zheng, H., et al., 2018. Using silicagel industrial wastes to synthesize polyethylene glycol/silica-hydroxyl form-stable phase change materials for thermal energy storage applications. Sol. Energ. Mat. Sol. Cells 178, 139–145. https://doi.org/10.1016/j.solmat.2018.01.016.

Sun, K.Y., Kou, Y., Zhang, Y.W., et al., 2020. Photo-triggered hierarchical porous carbon-based composite phase-change materials with superior thermal energy conversion capacity. ACS Sustain. Chem. Eng. 8, 3445–3453. https://doi.org/10.1021/acssuschemeng.9b07659.

Wang, J.W., Jia, X.L., Atinafu, D.G., et al., 2017. Synthesis of "graphene-like" mesoporous carbons for shape stabilized phase change material with high loading capacity and improved latent heat. J. Mater. Chem. A 5, 24321–24328. https://doi.org/10.1039/C7TA05594C.

Wang, Z.L., Zhang, H., Dou, B.L., et al., 2022. Effect of copper metal foam proportion on heat transfer enhancement in the melting process of phase change materials. Appl. Therm. Eng. 201,. https://doi.org/10.1016/j.applthermaleng.2021.117778 117778.

Xiao, S.K., Hu, X.W., Jiang, L., et al., 2022a. Nano-Ag modified bio-based loofah foam/polyethylene glycol composite phase change materials with higher photo-thermal conversion efficiency and thermal conductivity. J. Energy Storage 54,. https://doi.org/10.1016/j.est.2022.105238 105238.

Xiao, S.K., Zou, M.M., Xie, Y.Q., et al., 2022b. Nanosilver modified navel orange peel foam/polyethylene glycol composite phase change materials with improved thermal conductivity and photo-thermal conversion efficiency. J. Energy Storage 56,. https://doi.org/10.1016/j.est.2022.105976 105976.

Xu, J.H., Jiang, Y., Chen, X., et al., 2022. Photo- and magneto-responsive highly graphitized carbon based phase change composites for energy conversion and storage. Mater. Today Nano 19,. https://doi.org/10.1016/j.mtnano.2022.100234 100234.

Xu, Q., Liu, X.L., Luo, Q.Y., et al., 2021. Loofah-derived eco-friendly SiC ceramics for high-performance sunlight capture, thermal transport, and energy storage. Energy Storage Mater. 45, 786–795. https://doi.org/10.1016/j.ensm.2021.12.030.

Yuan, S.P., Wang, H.B., Li, X.Y., et al., 2022. Flame retardant and form-stable phase change composites based on phytic acid/dopamine-decorated delignified wood for efficient solar-thermal energy conversion and storage. Compos. A Appl. Sci. Manuf. 160,. https://doi.org/10.1016/j.compositesa.2022.107048 107048.

Zhang, Y., Wang, J.S., Qiu, J.J., et al., 2019. Ag-graphene/PEG composite phase change materials for enhancing solar-thermal energy conversion and storage capacity. Appl. Energy 237, 83–90. https://doi.org/10.1016/j.apenergy.2018.12.075.

Zhang, J.S., Zhang, X., Wan, Y.Z., et al., 2012. Preparation and thermal energy properties of paraffin/halloysite nanotube composite as form-stable phase change material. Sol. Energy 86, 1142–1148. https://doi.org/10.1016/j.solener.2012.01.002.